Particle Accelerators, 1992, Vols. 37–38, pp. 191–204
Reprints available directly from the publisher
Photocopying permitted by license only

STUDIES OF BEAM TRANSPORT, LONGITUDINAL COMPRESSION, AND RESISTIVE-WALL INSTABILITY AT THE UNIVERSITY OF MARYLAND†

M. REISER

Electrical Engineering Department and Laboratory for Plasma Research, University of Maryland, College Park, MD 20742.

(Received 19 December 1990)

This paper reviews the status of experiments at the University of Maryland electron beam facility that are relevant to Heavy Ion Inertial Fusion driver physics issues. In addition, the results of a new theoretical model on emittance growth in nonstationary beams are presented. The most important work so far has been the multiple-beam transport experiment in which the merging, image formation, and emittance growth due to charge nonuniformity of a five-beamlet configuration have been studied. The predictions of the new theory are found to be in excellent agreement with experimental observations and improved numerical simulation. Future work will involve the investigation of emittance growth due to initial mismatch and comparison with theory and simulation. A new electron-beam injector has been built and tested. It will be used to launch a new experimental program aimed at studying the physics of longitudinal compression and the longitudinal resistive-wall instability.

1 INTRODUCTION

At the University of Maryland, experiments designed to study the physics of space-charge-dominated (high-brightness) particle beams using low-energy electrons (5 kV, 40–260 mA) have been in progress for more than a decade. So far the main focus of this research has been the study of beam transport in a long periodic solenoid channel. As reported at the previous Heavy Ion Inertial Fusion Symposium at GSI Darmstadt[1], our early work was concerned with the maximum transportable beam current, I_{max}, and the limits imposed by envelope instabilities, and other effects. The experiments confirmed the theoretical predictions concerning I_{max} and the stability threshold of $\sigma_0 \leq 90°$ for the zero-current phase advance σ_0. We also reported at that meeting the results of our multiple-beam experiment, which is particularly relevant to Heavy Ion Inertial Fusion drivers using induction linacs. The first results of this experiment, which had been published earlier in *Physical Review Letters*[2], showed relatively good agreement among experiment, theory, and simulation with regard to the merging distance (≈ 15 cm). But the particle simulation point plots did not agree well in detail with the images observed on the fluorescent screen at larger distances from the source. Since then, I. Haber and H. Rudd have conducted a systematic

† Research supported by the U.S. Department of Energy.

search in parameter space to improve the simulation results. They finally obtained excellent agreement between simulation and experimental data by doubling the nominal initial emittance and by increasing the nominal magnetic field strength by 10%. A re-examination of the experimental parameters confirmed the correctness of the higher values for emittance and magnetic field. The results of this new work will be published in a separated paper.[3] A brief summary will be given in Section 2.

The equilibrium state of a charged particle beam in a linear focusing channel is a state of minimum energy and requires a uniform density profile if the beam is space-charge-dominated. The highly nonuniform distribution of a multiple beamlet configuration possesses an excess amount of field energy, which represents free energy that can be converted into emittance growth, as predicted by theory and simulation studies.[4–6] A new model has now been developed that improves the previous theory and includes other sources of free energy such as beam mismatch and off-centering. This work will be published elsewhere.[7] A brief summary of the new theory and the applications to the multiple-beam experiment will be presented in Section 3. Future experimental work will be concerned with studies of mismatched multiple beams and comparison with theory and simulation. Then our research direction will shift towards investigation of longitudinal pulse compression and longitudinal instability. An injector for this new phase has already been built. Its features and the parameters for the pulse compression experiments will be described in Section 4. The plans for longitudinal instability (resistive wall) studies will be reviewed in Section 5.

2 IMPROVED RESULTS FOR THE MULTIPLE BEAM EXPERIMENT

Past theoretical and numerical studies had shown that nonuniform charge distribution is a major cause of emittance growth in focusing channels. In 1987, we began an experiment to investigate this emittance growth, and the first results were published[2] in 1988. The nonuniform charge distribution we chose to study was a five-beamlet configuration formed by masking out a solid round beam. The beam was matched into the periodic solenoidal transport channel with two matching lenses. It then propagated along the 5-m long transport channel (consisting of 36 solenoid lenses) where numerous pictures were taken using a CCD camera. Figure 1 shows the multiple-beam experimental setup with the electron gun, the beam mask, the two matching lenses and the first lens of the long transport channel. The five beamlets were found to merge rather quickly in a distance of about 15 cm, as predicted by theory. Surprisingly, however, at a distance of 101 cm from the aperture plate, an image of the initial distribution was detected on the phosphor screen. No other image was found further down the channel. At the end of the channel, the beam was perfectly round, showing no spatial structure, and the emittance was measured using a slit/pinhole method. This experiment was completed in the spring of 1988. Particle simulation studies done in 1988 confirmed the merging effect, but there was very poor agreement with experiment on the image formation.[2]

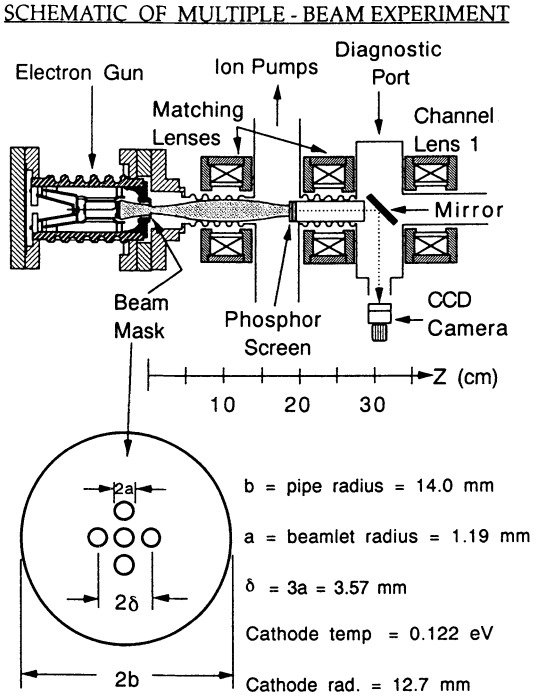

FIGURE 1 Schematic of the multiple-beam experimental setup.

The initial emittance ($\varepsilon_i \pi$) of the five-beamlet configuration is given by the equation

$$\varepsilon_i = R_i \left(\frac{2kT}{qV_0} \right)^{1/2}, \tag{1}$$

where

$$R_i = [a^2 - 1.6\delta^2] = 4.67 \text{ mm}. \tag{2}$$

Here, T is the temperature of the beam at the aperture plate, q the particle charge, V_0 the beam voltage, and k is Boltzmann's constant. R_i is the initial effective ($2 \times$ rms) radius of the five-beamlet configuration, $a = 1.19$ cm is the beamlet radius, and $\delta = 3a$ is the separation distance between the beamlet centers, as shown in Figure 1.

The magnetic field produced by a lens was represented by an analytical fit to the measured field profile on axis, and a Taylor expansion was used to obtain the nonlinear off-axis fields. The analytical on-axis field equation is given by

$$B(z) = B_0 \frac{\exp(-z^2/2b^2)}{1 + z^2/a^2}. \tag{3}$$

In this equation, a and b are fitting parameters and B_0 is the peak field value. The discrepancies in the simulations center around the value of temperature T in Eq. (1) and the values of B_0, a and b in Eq. (3).

In the original simulation studies that yielded poor agreement, the values of B_0, a, and b used were 83.2 gauss, 4.4 cm, and 2.29 cm, respectively. The initial temperature at the aperture plate used was the temperature of the cathode. It has been since recognized that the beam undergoes a compression of approximately a factor of two between the cathode and the aperture plate. As a result, there should be a corresponding increase in temperature by a factor of four and of the emittance by a factor of two. The value of emittance used in the original simulation which did not take beam compression into account was $\varepsilon_i\pi = 32.4\ \pi$ mm-mrad. By including the beam compression effect, one obtains the more accurate value of 64.8 π mm-mrad for the initial emittance of the five-beamlet configuration.

Even with this improved value for emittance, the simulation results remained poor. The location of the image and the Larmor beam rotation per period in the simulation did not match the corresponding image location and rotation in the experiment. The beam rotation can be inferred from the phosphor screen pictures, which are especially

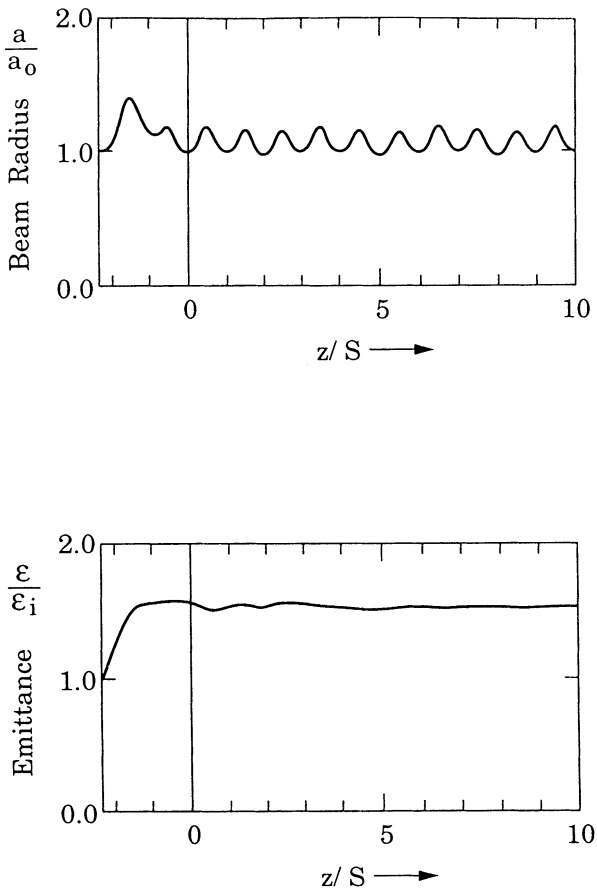

FIGURE 2 Numerical results for change of effective beam radius and emittance versus distance z in the multiple-beam experiment. S = 13.6 cm = length of one channel period.

clear at and near the image location of 101 cm downstream from the anode. When calculating the B_0 necessary to produce the observed rotation, it was found that the nominal value of B_0 had to be increased by 10% (i.e. from 83.2 gauss to 91.5 gauss). With this increased field strength very close agreement between simulation and experiment occurred. For reasons not yet fully understood, the nominal value assumed earlier for B_0 from field measurements was apparently too low. The details of these new results will be reported elsewhere.[3] Figure 2 shows the effective beam radius and emittance variation as obtained from the numerical simulation with the two times higher initial emittance and the 10% higher magnetic field. The emittance growth of 1.55, yielding a value of 100 π mm-mrad, is in reasonably good agreement with the measured emittance of 108 π mm-mrad at the end of the channel. Both the experimental and numerical results are also in excellent agreement with the new theory, as will be discussed in the next section.

3 NEW THEORY OF EMITTANCE GROWTH IN NONSTATIONARY BEAMS

In the stationary (equilibrium) state of a charged particle beam that is transported through a uniform or periodic linear focusing channel, the total transverse energy per particle, E, is at a minimum. If a beam is injected into the channel with a nonstationary density profile, with mismatched initial rms width (or slope), or off-centered, the total energy per particle is higher ($E + \Delta E$) than the energy of the equivalent stationary beam. The excess amount of energy, ΔE, in the nonstationary initial beam represents "free" energy that can be thermalized and thus converted into emittance growth.

According to the theory[7], if v is the particle velocity, $\gamma = (1 - v^2/c^2)^{-1/2}$ the relativistic energy parameter, m the particle mass, k_0 the external focusing constant and $a_i = 2x_{\text{rms}}$ the effective radius of the initial stationary beam, one can express the free energy in the form

$$\Delta E = \gamma m v^2 k_0^2 a_i^2 h. \tag{4}$$

The parameter h is a dimensionless constant that measures the free energy for any given case. In a periodic channel, k_0 is related to the zero-current phase advance per period, σ_0, and the period length, S, by

$$k_0 = \frac{\sigma_0}{S}. \tag{5}$$

An estimate of the possible emittance growth to conversion of free energy can be obtained by assuming that the nonstationary initial beam will evolve towards a final stationary state at the higher energy ($E + \Delta E$). If the focusing constant with space charge of the equivalent initial stationary beam is given and denoted by k_i, one can calculate the effective radius of the final stationary beam, a_f, from the relation[7]

$$\left(\frac{a_f}{a_i}\right)^2 - 1 - \left(1 - \frac{k_i^2}{k_0^2}\right) \ln \frac{a_f}{a_i} = h. \tag{6}$$

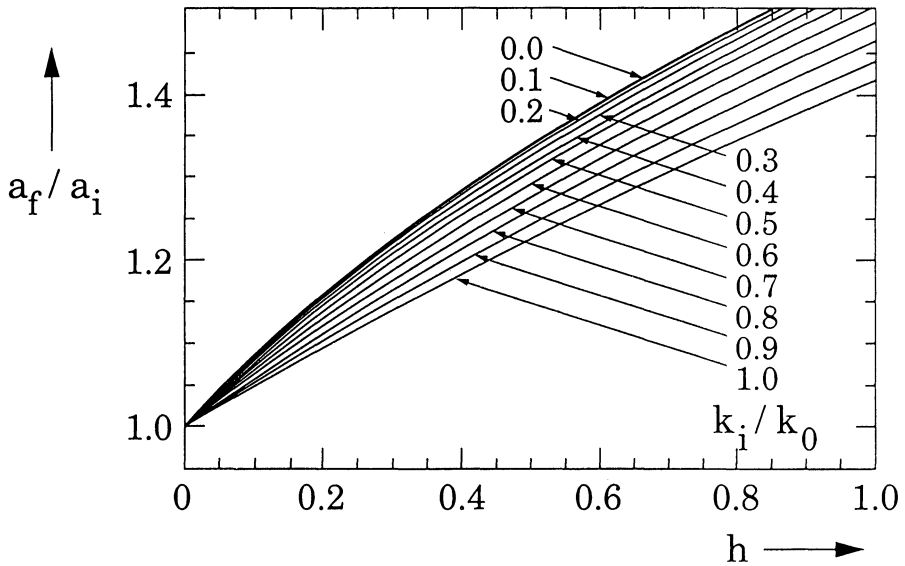

FIGURE 3 Ratio a_f/a_i of final and initial stationary beam radius versus the free-energy parameter h for different values of "tune depression" k_i/k_0.

For $a_f - a_i \ll a_i$, one obtains the results

$$\frac{a_f}{a_i} \approx 1 + \frac{h}{1 + k_i^2/k_0^2}. \tag{7}$$

Solutions of Eq. (6) are plotted in Figure 3, which shows a_f/a_i curves versus h for different values of k_i/k_0. By comparing the envelope equations for the final and initial stationary beams, one obtains for the emittance growth

$$\frac{\varepsilon_f}{\varepsilon_i} = \frac{a_f}{a_i}\left[1 + \frac{k_0^2}{k_i^2}\left(\frac{a_f^2}{a_i^2} - 1\right)\right]^{1/2}. \tag{8}$$

or in linear approximation ($a_f - a_i \ll a_i$)

$$\frac{\varepsilon_f}{\varepsilon_i} \approx \left(1 + 2\frac{k_0^2}{k_i^2} h\right)^{1/2}. \tag{9}$$

The free-energy parameter h was calculated for three cases, with the following results.[7]

Case 1 Nonuniform Charge Density Profile:

$$h = h_s = \frac{1}{4}\left(1 - \frac{k_i^2}{k_0^2}\right)\frac{U}{w_0}, \tag{10}$$

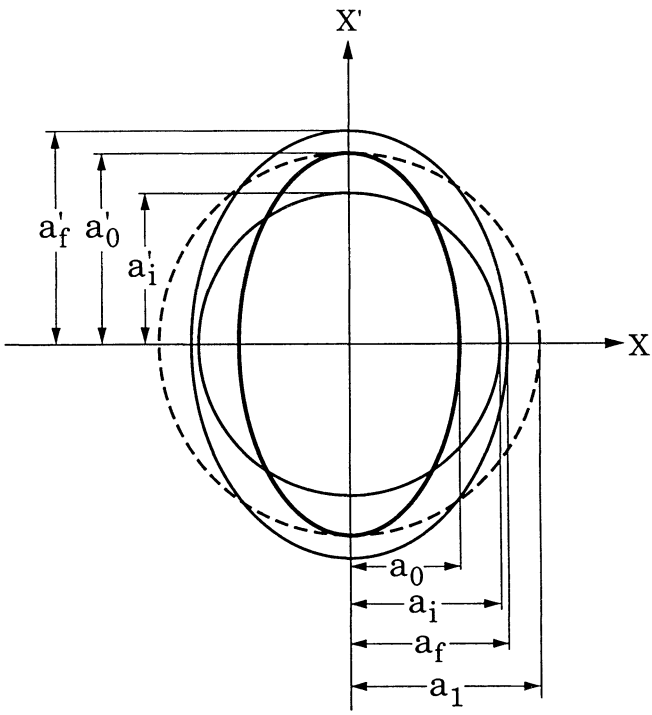

FIGURE 4 Phase-space ellipses for the initial mismatched beam (radius a_0, max. slope a'_0) and the corresponding "effective" emittance ($a_1 a'_0$), the initial stationary beam ($a_i a'_i$), and the final stationary beam ($a_f a'_f$).

where U/w_0 is the nonuniform field energy parameter defined in previous work.[2] This case was treated in the past with the assumption that the beam radius remains constant ($a_f \approx a_i$), and by substituting (10) in (9), one obtains the previous results.[4–6] However, in the general case when $a_f > a_i$, one must substitute h_s into (6) to find the radius ratio a_f/a_i, then use this result in Eq. (8) to obtain the emittance growth.

Case 2 Mismatched Beam

Figure 4 shows a mismatched initial phase-space ellipse in upright position (with radius a_0) and compares it with the equivalent initial matched beam ellipse (radius a_i), final matched beam ellipse (radius a_f), and the "effective" ellipse (radius a_1). The free energy parameter $h = h_m$ for this case can be calculated from the relation[7]

$$h_m = \frac{1}{2}\frac{k_i^2}{k_0^2}\left(\frac{a_i^2}{a_0^2} - 1\right) - \frac{1}{2}\left(1 - \frac{a_0^2}{a_i^2}\right) + \left(1 - \frac{k_i^2}{k_0^2}\right)\ln\frac{a_i}{a_0}. \tag{11}$$

In conventional theory, where space charge is neglected, nonlinearities in the external focusing field produce distortions in the mismatched beam ellipse, so that

after several betatron periods the beam essentially fills the entire area of the effective ellipse. This effective emittance growth is given by

$$\frac{\varepsilon_{\text{eff}}}{\varepsilon_i} = \frac{a_1}{a_0}, \tag{12}$$

where a_0 is the radius of the mismatched beam at the waist and a_1 is the corresponding radius at the maximum of the mismatched beam envelope.

By comparison, the emittance growth [Eq. (8)] of a space-charge dominated beam can be considerably greater than that given by Eq. (12) depending on the degree of mismatch and the "tune depression" k_i/k_0.

Case 3 Off-Centered Beam

Assume that the initial beam centroid is off-centered in the x-direction by an amplitude x_c. Then it is easy to show that the free energy parameter $h = h_c$ is given by[7]

$$h_c = \frac{x_c^2}{a_i^2}\frac{k_c^2}{k_0^2}. \tag{13}$$

If two or all three of the above effects are present, then the total emittance growth can be calculated from the sum of the free energy parameters

$$h = h_s + h_m + h_c. \tag{14}$$

Let us now apply the above theoretical results to the multiple-beam experiment described in Section 3. Figure 5 shows the results of the numerical simulation for the matched nonuniform beam.[3] To compare with the new theory, we must first calculate the average radius, a_i, of the equivalent stationary beam having the same current and emittance as the initial nonstationary beam, but uniform current density. From the smooth approximation theory[8] one finds

$$a_i = (\varepsilon_i S/\sigma_0)^{1/2}[u + \sqrt{1+u^2}]^{1/2}, \tag{15}$$

where $u = KS/2\sigma_0\varepsilon_i$.

The relevant parameter values are $S = 13.6$ cm, $K = 1.877 \times 10^{-3}$, $\varepsilon_i = 64.8$ mm-mrad ($2\times$ original value), $\sigma_0 = 76.3°$ (for 10% higher B-field and compared to original value of 70°). With these values, Eq. (15) yields

$$a_i = 4.65 \text{ mm}. \tag{16}$$

The tune depression $k_i/k_0 = \sigma_i/\sigma_0$ is found from the smooth-approximation relation[8]

$$\frac{Ka_i^2}{\varepsilon_i^2} = \frac{\sigma_0^2}{\sigma^2} - 1 \tag{17}$$

yielding

$$\frac{\sigma_0}{\sigma_i} = 3.26, \quad \text{or} \quad \frac{\sigma_i}{\sigma_0} = \frac{k_i}{k_0} = 0.3. \tag{18}$$

The parameter U/w_0 was calculated[2] to be $U/w_0 = 0.2656$, hence one finds for the free energy parameter for our five-beamlet configuration from Eq. (10):

$$h_s = 0.06, \tag{19}$$

yielding for the radius ratio

$$\frac{a_f}{a_i} = 1.055 \tag{20}$$

and for the emittance growth

$$\frac{\varepsilon_f}{\varepsilon_i} = 1.56. \tag{21}$$

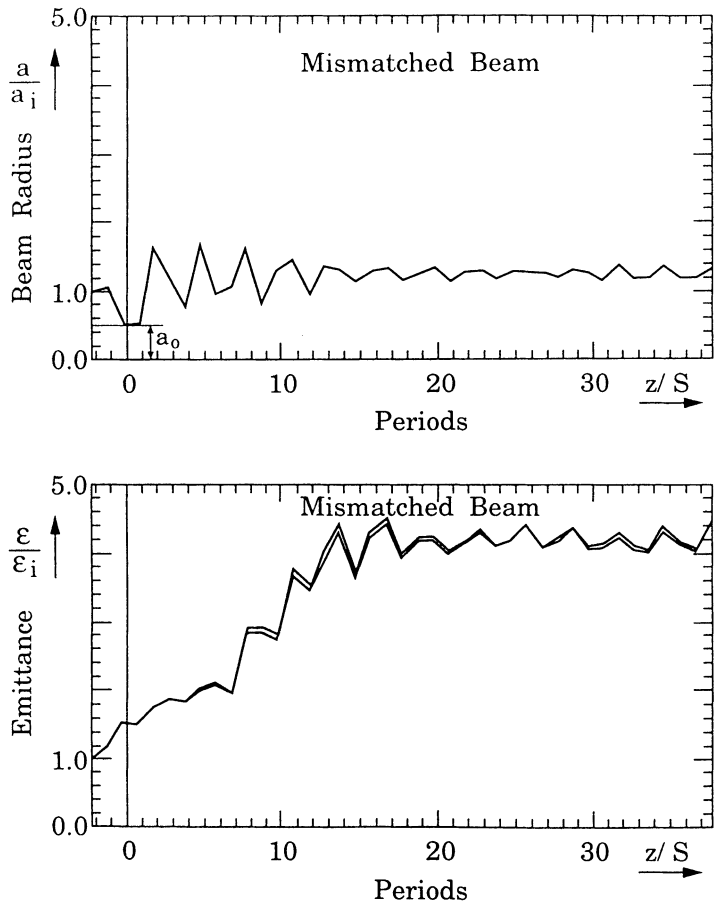

FIGURE 5 Numerical results for change of effective beam radius and emittance versus number of channel periods when multiple beam configuration is injected with a mismatch of $a_0/a_i = 0.5$.

These values are in excellent agreement with the simulation results shown in Figure 2, which compared well with the experimental data, as already discussed.

To further compare the new theory with simulation a computer run was performed by H. Rudd for the case of a mismatched five-beamlet configuration with initial radius $a_0 \approx 0.5a_i$. The results for beam radius and emittance growth versus channel distance are plotted in Figure 5. The theory yields

$$h_m = 0.4, \tag{22}$$

$$\frac{a_f}{a_i} = 1.28, \tag{23}$$

and

$$\frac{\varepsilon_f}{\varepsilon_i} = 3.72. \tag{24}$$

For the total emittance due to the space charge nonuniformity and the mismatch one obtains

$$\left(\frac{\varepsilon_f}{\varepsilon_i}\right)_{\text{total}} = \left(\frac{\varepsilon_f}{\varepsilon_i}\right)_{\text{total}} = 3.8. \tag{25}$$

The results of Eqs. (24) and (25) are remarkably close to the final simulation values for the beam radius and emittance growth in Fig. 5. It is interesting that this "thermalization" of the free energy and the approach to a new stationary state occurs in less than half of the channel distance. Also the effect is very significant. We therefore plan to conduct experiments with mismatched beams in order to check the validity of the predictions from theory and simulation.

4 LONGITUDINAL COMPRESSION EXPERIMENTS

A new electron beam injector was built and tested for studies of longitudinal compression in our solenoid channel. This injector consists of a gridded electron gun to vary the beam perveance and pulse width, an induction acceleration module to impart a head-to-tail energy shear (2.5 to 7.5 keV) for pulse compression, and three solenoid lenses to match the beam into the channel. The electron gun, whose design and performance characteristics have been described elsewhere[9], produces beam pulses ranging from a few nanoseconds to about 50 ns in time duration, with peak currents between 20 and 160 mA. The emittance is in the range of 60–80 π mm-mrad which is small enough so that the beam is dominated for the most part by space-charge forces.

The induction module has been tested, and the time variation of the induced acceleration voltage $V(t)$ is close to the desired quadratic shape needed to produce a linear velocity shear across the 40 ns electron pulse. Details can be found elsewhere.[10]

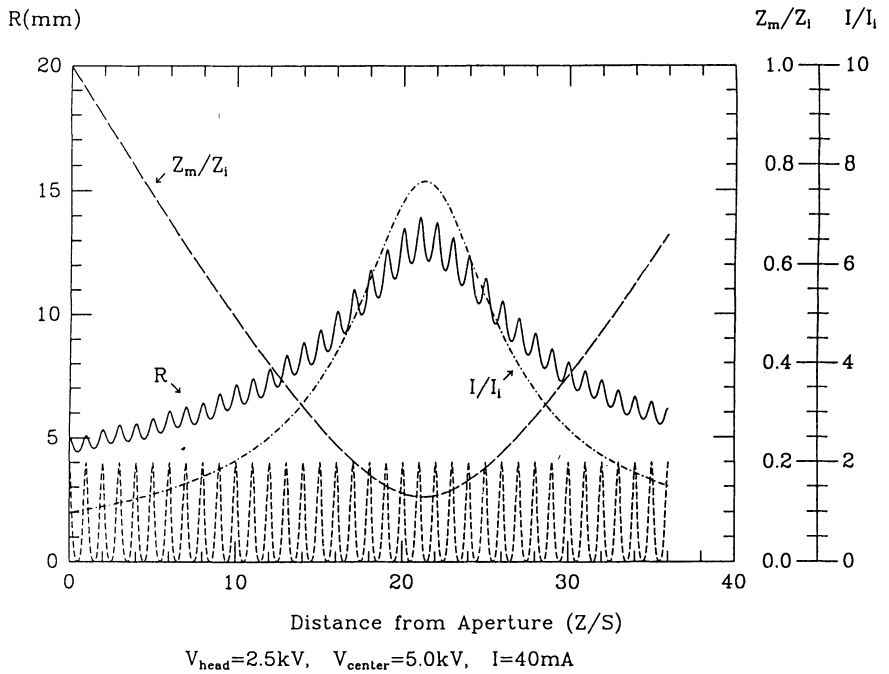

FIGURE 6 Variation of pulse length z_m/z_i, beam peak current, I/I_i, and radial width of pulse center (5 kV), R, versus number of periods in periodic solenoid channel. (From simultaneous integration of longitudinal and transverse envelope equations as described in Ref. 11.) The phase advance without space charge for 5 kV particles at center of pulse was assumed to be $\sigma_0 = 70°$.

The goals for the pulse compression experiment have been described in a paper at the 1989 IEEE Particle Accelerator Conference.[11] They are illustrated in Figure 6, which displays the results of simultaneous integration of the K–V envelope equation for the radius of the beam center and the longitudinal envelope equation. The figure shows in a qualitative way the behavior of the 40-mA, 2.5-keV, 40-ns beam pulse from the electron gun in the solenoidal focusing channel. After passage through the induction module, the beam head remains at 2.5 keV, the center has an energy of 5 keV, and the tail (not shown) has an energy of 7.5 keV. The energy shear in this particular case leads to a longitudinal compression, z_i/z_m, and concurrent current increase, I/I_i, by a factor of about 7.7. The point of maximum compression occurs at a distance of about 21 lens periods from the channel entrance. After that, the beam expands again longitudinally. The radial width of the beam at the center of the pulse increases (due to the changing current) from 5 mm initially to about 13 mm at maximum compression; after that it decreases again, as expected.

The major goal of the experiment is to study the compression physics, in particular the emittance growth that may occur due to longitudinal-transverse coupling, nonlinear forces, and other effects. An understanding of longitudinal compression is essential for Heavy Ion Inertial Fusion, where bunching of long-pulse, low-current

beams is a major feature of the accelerator-driver systems to achieve the high-power, short-pulse beams required for igniting the target.

5 LONGITUDINAL RESISTIVE-WALL INSTABILITY STUDIES

The longitudinal resistive-wall instability is a major concern for the induction linac in Heavy Ion Inertial Fusion. It occurs due to the fact that the impedance per unit length, $Z_w = R + iX$, of the induction-acceleration gap seen by the beam has a relatively high resistive component ($R \approx 100\,\Omega$/m). As a result, slow space-charge waves produced by current perturbations and traveling backwards in the beam frame are unstable. The amplitudes of such waves increase with distance and cause momentum spread that exceeds the requirements for final focusing. In a sense, the effect is similar to that of a purely resistive wall in which beam energy is dissipated due to ohmic losses of the induced currents. The theory of this instability, which is well known, is extended in a separate paper[12] to include the effects of capacitive and inductive components of the wall impedance Z_w. For a purely resistive wall, one finds exponential growth, $e^{\omega_i t}$, with a growth rate of

$$\omega_i = \frac{1}{2} v_0 R \left(\frac{4\pi\varepsilon_0}{g} \frac{q\lambda_0}{m} \right)^{1/2} = \frac{1}{2} v_0 R \left(\frac{4\pi\varepsilon_0}{g} \frac{qI}{mv_0} \right)^{1/2}, \tag{26}$$

where $\lambda_0 = I/v_0$ denotes the charge per unit length, v_0 the beam velocity, I the beam current, and

$$g = \frac{2}{3} + 2ln \frac{b}{a} \tag{27}$$

the geometry factor, with b/a defining the ratio of wall radius to beam radius. The distance for an e-fold increase of the amplitude of the unstable slow wave is given by $l_e = v_0/\omega_i$, or

$$l_e = \frac{2}{R} \left(\frac{g}{4\pi\varepsilon_0} \frac{mv_0}{qI} \right)^{1/2}. \tag{28a}$$

For heavy ions with charge $q = Ze$, mass $m = Am_p$, and particle current $I_p = I/Z$, it is convenient to write this relation in the form

$$l_e = \frac{2}{R} \left(\frac{30gAm_pc^2\beta}{Z^2eI_p} \right)^{1/2}, \tag{28b}$$

where $\beta = v_0/c$.

For $R = 100\,\Omega$/m, $g \simeq 2$, $A = 200$, $Z = 3$, $I_p = 10$ kA, and $\beta = 0.3$, one finds $l_e \approx 120$ m. This distance is very short compared to the total length of the accelerator and final transport (5–10 km). Hence, measures must be taken to minimize and correct the effects of the instability. On the other hand, an e-fold distance of $\gtrsim 100$ m is too long to do realistic experiments with heavy ion beams since an appropriate facility

is very costly and not yet available. Consequently, much of the design work must rely on modeling and the use of computer codes.

Since the e-fold growth length is proportional to $(m/q)^{1/2}$, experiments with electron beams are an attractive alternative to study the instability. We are proposing to do such studies with our electron beam facility at the University of Maryland. With our 5-keV ($\beta = 0.14$), 100-mA beam, and assuming a resistive wall of 10 kΩ/m, one obtains an e-fold distance of $l_e = 1.3$ m, which is about a quarter of the length of our periodic solenoid channel. The resistive wall can be built by coating a glass pipe with tin oxide, following the pioneering work of Birdsall *et al.* on the resistive-wall amplifier.[13] Further details of our work, regarding both the theory and the conceptual design of the proposed experiment, can be found in our other paper.[12] Since we can produce rather short pulses (5 ns, or approximately 15 cm in length) with our new electron gun, it would be possible to observe the reflection of the slow wave from the rear end of the pulse if the beam were propagated over a distance of several meters. The wave reflections at the bunch ends are not yet fully understood, and the proposed experimental investigation would be very valuable in providing information and for testing computer codes.

6 CONCLUSIONS

The electron beam facility at the University of Maryland has become a valuable research tool to study the transport of high-brightness beams and to compare theory and particle-simulation results with experimental data. Particularly relevant to Heavy Ion Inertial Fusion driver design is the multiple-beam experiment and the new theory on emittance growth in nonstationary beams. The remarkably good agreement between theoretical predictions, numerical simulation, and experimental observation is of great significance. It proves that the theory and the simulation code can be used to predict beam behavior and to design heavy-ion driver experiments.

The longitudinal compression experiment, for which the new injector has already been tested, and the proposed resistive-wall instability experiment could serve a similar purpose for the study of longitudinal beam physics. The electron beam facility can provide an inexpensive testbed for checking theory and computer simulation codes and for obtaining information on beam behavior in a laboratory environment.

REFERENCES

1. M. Reiser, *Nucl. Instrum. Meth. A* **278**, 138 (1989).
2. M. Reiser, C. R. Chang, D. Kehne, K. Low, T. Shea, H. Rudd, and I. Haber, *Phys. Rev. Lett.* **61**, 2933 (1988).
3. I. Haber, D. Kehne, M. Reiser, and H. Rudd, "Experimental, Theoretical and Numerical Investigation of the Homogenization of Current Nonuniformities in the Periodic Transport of Space-Charge Dominated Beams," to be published in *Phys. Rev. A.*
4. J. Stuckmeier, J. Klabunde, and M. Reiser, *Part. Accel.* **15**, 47 (1984).
5. T. P. Wangler, K. R. Crandall, R. S. Mills, and M. Reiser, *IEEE Trans. Nucl. Sci.* **32**, 2196 (1985).
6. O. A. Anderson, *Part. Accel.* **21**, 197 (1987).
7. M. Reiser, "Free Energy and Emittance Growth in Nonstationary Charged Particle Beams," *J. Appl. Phys.* **70**, 1919 (1991).

8. M. Reiser, *Part. Accel.* **8**, 167 (1978).
9. J. G. Wang, E. Boggasch, P. Haldemann, D. Kehne, M. Reiser, T. Shea, and D. X. Wang, *IEEE Trans. Elect. Devices* **37**, 2622 (1990).
10. J. G. Wang, D. X. Wang, E. Boggasch, D. Kehne, M. Reiser, and T. Shea, *Nucl. Instrum. Meth. A* **301**, 19 (1991).
11. T. Shea, E. Boggasch, Y. Chen,. M. Reiser, *Proc. 1989 IEEE Part. Accel. Conf.* IEEE publication 89CH2669-0 p. 1049.
12. J. G. Wang, M. Reiser, W. M. Guo, and D. X. Wang, *Part. Accel.* **37–38**, 181 (1991).
13. C. K. Birdsall, G. R. Brewer, A. V. Haeff, Proc. of the I.R.E. **41**, 865 (1953).